Chapter 1
Diabetic Macular Edema

Conceição Lobo, Isabel Pires, and José Cunha-Vaz

Abstract The optical coherence tomography (OCT), a noninvasive and noncontact diagnostic method, was introduced in 1995 for imaging macular diseases.

In diabetic macular edema (DME), OCT scans show hyporeflectivity, due to intraretinal and/or subretinal fluid accumulation, related to inner and/or outer blood–retinal barrier breakdown. OCT tomograms may also reveal the presence of hard exudates, as hyperreflective spots with a shadow, in the outer retinal layers, among others.

In conclusion, OCT is a particularly valuable diagnostic tool in DME, helpful both in the diagnosis and follow-up procedure.

1.1 Introduction

The World Health Organization (WHO) estimates that more than 180 million people worldwide have diabetes, and this number is expected to increase and to rise to epidemic proportions within the next 20 years [1]. Diabetic retinopathy, one of the most frequent complications of diabetes, remains a major public health problem with significant socioeconomic implications, affecting approximately 50% of diabetic subjects, and remains the leading cause of blindness in working-age populations of industrialized countries.

Diabetic macular edema (DME) is the largest cause of visual acuity loss in diabetes [2]. It affects central vision from the early stages of retinopathy, and it is the

C. Lobo (✉)
AIBILI-Association for Innovation and Biomedical Research on Light and Image,
Azinhaga Santa Comba, 3000-548 Coimbra, Portugal
e-mail: clobo@aibili.pt

R. Bernardes and J. Cunha-Vaz (eds.), *Optical Coherence Tomography*,
Biological and Medical Physics, Biomedical Engineering,
DOI 10.1007/978-3-642-27410-7_1,

most frequent sight-threatening complication of diabetic retinopathy, particularly in older type 2 diabetic patients. Its role in the process of vision loss in diabetic patients and its occurrence in the evolution of the retinal disease are being increasingly recognized.

DME leads to distortion of visual images and may cause a significant decrease in visual acuity even in the absence of severe retinopathy.

Although macular edema is a common and characteristic complication of diabetic retinopathy and shows apparent association with the systemic metabolic alterations of diabetes, it does not necessarily fit the regular course of diabetic retinopathy progression. It may occur at any stage of diabetic retinopathy, whether nonproliferative, moderate, or severe, or even at the more advanced stages of the retinopathy [3].

These facts are particularly important regarding the relevance of DME in the natural history of diabetic retinopathy. Diabetic retinopathy often progresses for many years without vision loss, making it sometimes challenging for the physician to counsel the patient for the need for treatment when progression occurs.

1.2 Pathophysiology of Retinal Edema

Retinal edema occurs when there is an increase of water in the retinal tissue, resulting in an increase in its thickness. This increase in water content of the retinal tissue may be initially intracellular (cytotoxic edema) or extracellular (vasogenic edema) [4]. In DME, extracellular edema resulting from breakdown of the blood–retinal barrier (BRB) is generally present.

In the retina, there is a specialized structure, the BRB, that regulates fluid movements into and out of the retinal tissue. If the BRB breaks down, as occurs in diabetes, it results in an "open BRB", which enables increased movements of fluids and molecules into the retina, with extracellular accumulation of fluid and deposition of macromolecules.

1.3 Extracellular Edema

Extracellular edema is directly associated with a situation of "open BRB" [4]. In this situation, the increase in tissue volume is due to an increase in the retinal extracellular space. Breakdown of the BRB is well identified by fluorescein leakage, which can be detected in a clinical environment by fluorescein angiography or vitreous fluorometry measurements. In this type of edema, Starling's law governing the movements of fluids applies [5].

1.4 Starling's Law

In extracellular edema, the "force" driving water across the capillary wall is the result of a hydrostatic pressure difference ΔP and an effective osmotic pressure difference $\Delta\pi$. The equation regulating fluid movements across the BRB is, therefore

$$\text{Driving\_force} = \text{Lp}\,[(\text{Pplasma} - \text{Ptissue}) - \sigma\,(\pi\text{plasma} - \pi\text{tissue})]$$

where Lp is the membrane permeability of the BRB, σ is an osmotic reflection coefficient, Pplasma is blood pressure, and Ptissue is the retinal tissue osmotic pressure.

An increase in ΔP, contributing to retinal edema, may be due to an increase in Pplasma and/or a decrease in Ptissue. An increase in Pplasma due to increased systemic blood pressure contributes to retinal edema formation only after loss of autoregulation of retinal blood flow and alteration of the structural characteristics of the BRB. A decrease in Ptissue is an important component that has not been given sufficient attention. Any loss in the cohesiveness of the retinal tissue due to pathologies such as cyst formation, vitreous traction, or pulling at the inner limiting membrane will lead to a decrease in Ptissue. A decrease in Ptissue, i.e., increased retinal tissue compliance, may lead to fluid accumulation, edema formation, and an increase in retinal thickness.

A decrease in $\Delta\pi$, contributing to retinal edema, may occur due to increased protein accumulation in the retina after breakdown of the BRB. Extravasation of proteins will draw more water into the retina. This is the main factor provoking a decrease in $\Delta\pi$, as a reduction in plasma osmolarity high enough to contribute to edema formation is an extremely rare event.

After a breakdown of the BRB, the progression of retinal edema depends directly on the ΔP and $\Delta\pi$ gradients. In these situations, tissue compliance becomes more important, influencing directly the rate of edema progression.

Thus, in the presence of retinal edema, it is essential to recognize the presence of an "open BRB" [6].

1.5 Incidence and Prevalence of DME

The incidence and prevalence of DME have been reported in different epidemiologic studies with significant variations, depending on the type (type I or II), treatment (insulin, oral hypoglycemic agents, or diet only), and the mean diabetes duration. Although DME can develop at any stage of DR, it is frequently related with increase in duration and severity of DR.

DME prevalence, indicated in the Wisconsin Epidemiologic Study in Diabetic Retinopathy (WESDR), is only about 3% in mild nonproliferative diabetic retinopathy (NPDR), but increases to 38% in moderate to severe NPDR and to 71% in eyes with proliferative diabetic retinopathy (PDR). In this study, the incidence of

clinically significant DME was 4.3% in type I diabetic patients and 5.1% in type II with insulin and 1.3% in those without insulin. At 10 years, the rate of developing DME was 20.1% in patients with diabetes type I and 25.4% in type II diabetic patients needing insulin and 13.9% in those without insulin [7].

1.6 Clinical Evaluation of Macular Edema

Clinical evaluation of macular edema has been characterized by its difficulty and subjectivity. Direct and indirect ophthalmoscopy may only show an alteration of the foveal reflexes. Stereoscopic fundus photographs (SFP) and slit-lamp fundus stereo biomicroscopy have been the standard clinical methods to evaluate changes in retinal volume in the macular area, but they are dependent on the observer experience, and the results do not offer a reproducible measurement of the volume change [5]. Nevertheless, together they are useful to visualize signs correlated with retinal thickening, such as hard and soft exudates, hemorrhages, and microaneurysms.

The introduction of imaging methods, such as optical coherence tomography (OCT), made macular edema evaluation more precise and reliable.

1.7 Diagnosis and Classification

The Early Treatment Diabetic Retinopathy Study Group (ETDRS) defined DR severity stages [8] and DME [9] based on clinical grounds by SFP. DME is an increase in retinal thickness at or within 1 disk diameter of the foveal center, whether focal or diffuse, with or without hard exudates, sometimes associated with cysts. In this study, the term "clinically significant macular edema" (CSME) was introduced to characterize the severity of the disease and to provide a threshold level to apply laser photocoagulation. Three different CSME situations can occur:

1. Increase in retinal thickness $\leq$500 μm of the center of the fovea
2. Hard exudates $\leq$500 μm of the center of the fovea with increased retinal thickness
3. Increase in retinal thickness $\geq$1 disk diameter with at least one part within 1 disk diameter at the center of the fovea

Fluorescein angiography (FA) has been an important method to evaluate DME, and although not considered a screening exam, it provides important information about retinal perfusion, blood–retinal barrier integrity, and new vessel growth.

Angiographic classifications of DME have included noncystoid and cystoid macular edema (CME) [10] and focal or diffuse DME [11,12]. Focal macular edema is characterized by the presence of localized areas of retinal thickening associated with focal leakage of individual microaneurysms or clusters of microaneurysms or dilated capillaries. Diffuse macular edema is a more generalized and chronic form

of edema, visualized as widespread macular leakage and pooling of dye in cystic spaces [13].

Ophthalmoscopy, SFP, and FA have been for many years the traditional methods used to evaluate diabetic retinopathy and DME, although they do not provide neither quantitative measurements of retinal thickness nor information about cross-sectional retinal morphology.

Recently, one methodology capable of measuring objective changes in retinal thickness and giving morphological and topographic surface images became available, the OCT, changing dramatically the landscape of DME diagnostic and follow-up.

OCT is a noninvasive and noncontact diagnostic method, well tolerated by patients, that provides important information about the retina. OCT imaging is analogous to B-scan ultrasound imaging, except that it uses infrared light reflections instead of ultrasound. It produces reliable, reproducible, and objective cross-sectional images of the retinal structures and the vitreoretinal interface and allows quantitative measurements of retinal thickness (RT). Since its commercial introduction in 1995, it enhanced the ability to diagnose and guide treatment decisions in retinal pathology, namely, macular holes, DME, epiretinal membranes, choroidal neovascularization, and vitreomacular traction, and thus became a powerful tool, widely used, for research and clinical evaluation of retinal disease.

OCT brought new insights about morphological changes of the retina in diabetic retinopathy and DME. It showed that macular edema may assume different morphologic patterns [14,15]. In addition, a quantitative characterization of macular edema became feasible, as determined by measurements of retinal thickness and volume. OCT has been demonstrated to be more sensitive than slit-lamp biomicroscopy in detecting small changes in retinal thickness [16–19] and is clearly less subjective. In cases of DME, OCT scans may demonstrate diffuse thickening of the neurosensory retina and loss of the foveal depression; cystic retinal changes, which manifest as areas of low intraretinal reflectivity; and serous retinal detachment, alone or combined.

Over the last decade, the development of OCT instrumentation progressed rapidly. The first and second generations of commercial OCT instrument time domain (TD) (OCT1, OCT2) had an axial resolution of 10–15 μm. Third generation OCT (OCT3, Stratus; Carl Zeiss Meditec, Dublin, California, USA) provided an axial resolution of 8–10 μm. The recently available spectral-domain OCT (SD-OCT) has an axial resolution of 5–6 μm and has almost 100-fold improvement in acquisition speed over conventional time-domain OCT scanners since the moving reference arm is eliminated and all data points can be analyzed simultaneously. With increased imaging speed and greater signal-to-noise ratio, SD-OCT scanners produce more detailed and brighter images, with greater detail. Consequently, it is possible to decrease the motion artifacts and obtain a more precise registration from a larger area to be scanned. It is also possible to obtain an in vivo three-dimensional (3D) imaging that allows correlation between OCT images and clinical fundus features.

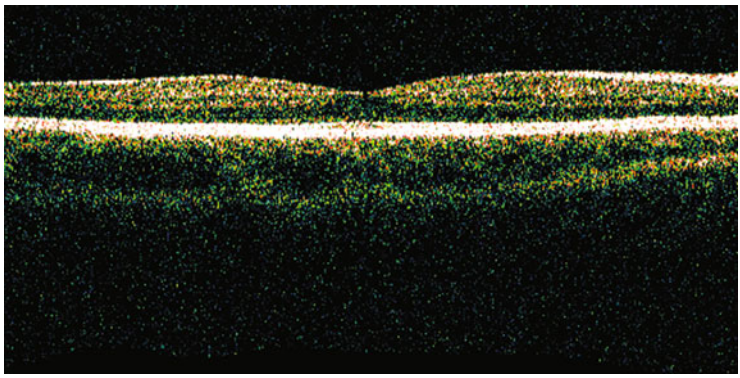

Fig. 1.1 TD-OCT, Stratus: normal cross-sectional macular image

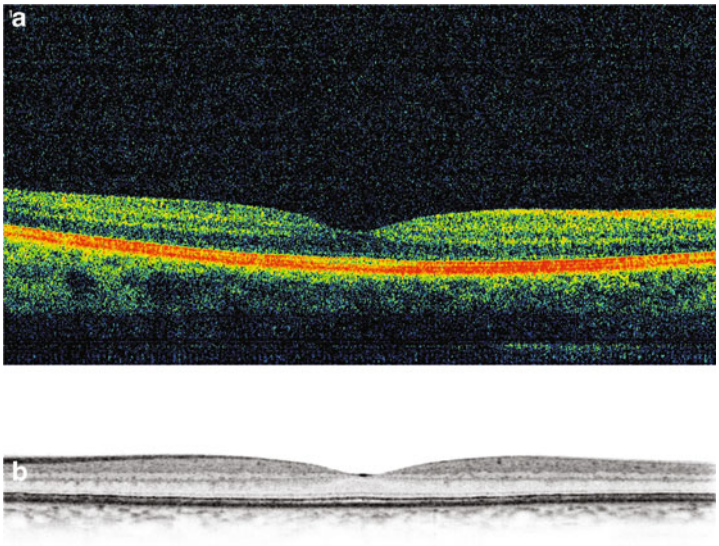

Fig. 1.2 SD-OCT, Cirrus: normal cross-sectional macular image; (**a**) false color; (**b**) gray scale

Cross-sectional images resemble closely the histological appearance of the retina [20] (Figs. 1.1–1.4). The top of the image corresponds to the vitreous cavity, which is optically silent, in a normal patient, or may show the posterior hyaloidal face, if there is a posterior vitreous detachment [21]. Central foveal depression is visible in normal eyes. The anterior boundary of the retina corresponds to the internal limiting membrane (ILM), at the vitreoretinal interface, hyperreflective and well defined, because of the contrast between the nonreflective vitreous and the backscattering of the retina.

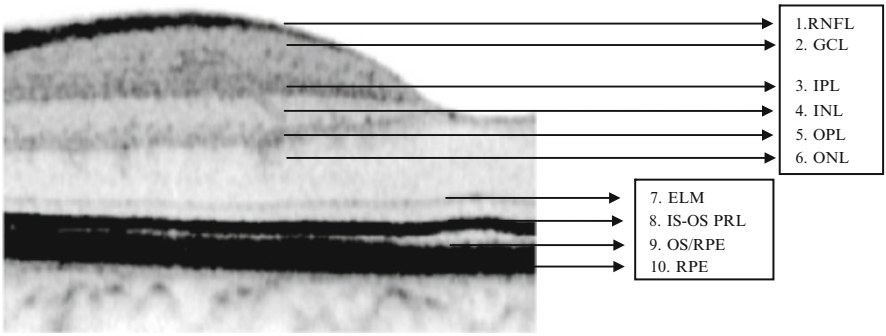

Fig. 1.3 SD-OCT, Spectralis: normal cross-sectional macular image (gray scale) and anatomic correlation. (1) RNFL, (2) GCL, (3) IPL, (4) INL, (5) OPL, (6) ONL, (7) ELM, (8) IS-OS PRL, (9) OS/RPE junction, and (10) RPE

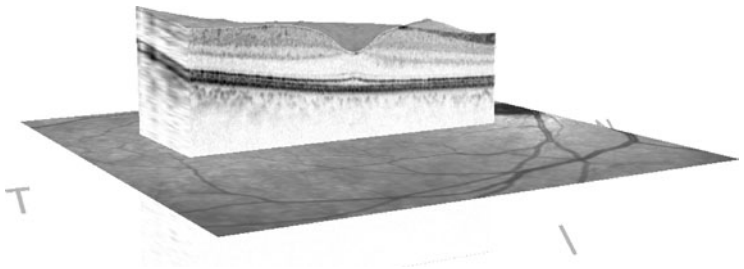

Fig. 1.4 SD-OCT, Spectralis: 3D image of RT from a healthy volunteer

The internal structure of the retina has heterogeneous reflections and distinct bands, and an anatomic correlation with the layers of the human retina has been proposed [22] (Fig. 1.3). Retinal nerve fiber layer (RNFL) is aligned horizontally, demonstrating higher tissue signal strength and appears thicker closer to the optic nerve, as expected. Axially aligned cellular layers—ganglion cell layer, inner nuclear layer, and outer nuclear layer (GCL, INL, and ONL, respectively)—have lower tissue signal compared with horizontally aligned layers, ILM, RNFL, and plexiform layers, which have higher tissue signal. Typically, nuclear layers appear hyporeflective, while plexiform layers (inner plexiform layer and outer plexiform layer—IPL and OPL, respectively) and axonal layers are relatively hyperreflective.

In the outer retina, different hyperreflective structures (bands) are visualized. TD Stratus OCT image shows the outer retinal layers as two hyperreflective bands, the photoreceptor's outer segments (inner) and the RPE/choriocapillaris complex (outer). On the other hand, SD-OCT scans of the outer retina allow the visualization of more bands than the TD-OCT. With this high resolution technology, 3 or 4 distinct strongly reflective bands are apparent, although their histological correlation remains a matter of discussion. According to Pircher et al. [23], the first (inner) band may correspond to the external limiting membrane (ELM),

the second to the interface of the inner and outer segments (IS-OS) of the photoreceptor layer (IS-OS PRL), the third band may represent the outer segment-RPE junction (OS-RPE), and the fourth (outer) is assumed to represent the RPE (Fig. 1.3). The separation between the third and the fourth hyperreflective lines may not always be visible [23]. The analysis of structural changes in the outer retinal layers, particularly affecting photoreceptors and their interface, is now possible, using SD-OCT scanners [24]. In fact, the disruption of the photoreceptor IS/OS junction appears to be an important indicator of photoreceptor integrity or impairment and visual acuity outcome, as highlighted in several recent studies on distinct retinal diseases, such as branch retinal vein occlusion [25], central serous chorioretinopathy [26], retinitis pigmentosa [27], type 2 idiopathic macular telangiectasia (IMT) [28, 29], and DME [30, 31]. A recent report showed a strong correlation of photoreceptor's outer segments length, measured with Cirrus SD-OCT, and visual acuity, in DME [32].

Initial studies found a good correlation between macular thickening, assessed with OCT, and visual acuity [15, 33–35]. However, recent reports show only a moderate correlation between central retinal thickness and visual acuity, in patients with DME [36,37], implying that visual acuity may depend mainly on the disruption of the retinal architecture or direct photoreceptor damage.

The possibility to quantify retinal thickness by OCT is based in the distance between the anterior and posterior highly reflective boundaries of the retina, using appropriate algorithms [38]. All instruments identify the vitreoretinal interface as the inner retinal border; however, the segmentation of the outer retinal border differs widely among different OCT instruments. While the Stratus OCT system uses the photoreceptor's outer segments band for segmentation, spectral OCT devices use the second or the fourth hyperreflective lines as the outer border of the retina. As a consequence, Stratus OCT generates lower values of retinal thickness, while spectral-domain technology gives higher thickness values.

Since the commercialization of OCT systems, several types of software to quantify macular thickness became available. The first version (OCT 1, OCT 2—Carl Zeiss Meditec, Humphrey Division, Dublin, CA, USA) and, later, Stratus OCT (Carl Zeiss Meditec, Humphrey Division, Dublin, CA, USA) comprised automated macular thickness acquisition protocols consisting of six radial line scans, approximately 6 mm long each, obtained in a spoke-like pattern centered on the fovea (radially). Retinal thickness is measured along these six intersecting lines, with the advantage of concentrating measurements in the central fovea [38]. The high-density scanning protocol of the Stratus OCT (software version 4.0) uses six radial lines of 6 mm (B-scan), each containing 128 A-scans, with a total of 768 A-scans. Acquisition time for the scan is 1.5 s. Mean macular retinal thickness (RT) is displayed as a two-dimensional false color-coded map, where bright colors (e.g., red and white) represent thick areas and dark colors (e.g., blue and black) represent thin areas, and as a numerical map, for nine ETDRS-type areas (Fig. 1.5). Average RT is calculated automatically for each of the nine quadrants. Because data point density is greater centrally than peripherally, interpolated thickness measurements

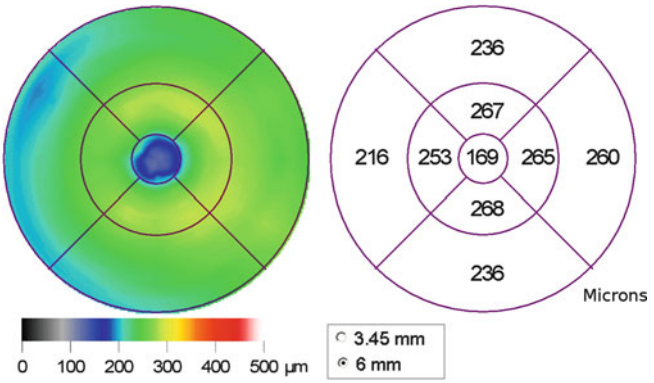

Fig. 1.5 TD-OCT, Stratus: two-dimensional color-coded RT map and its numerical representation from a healthy volunteer

of regions farther from the fovea are determined from fewer measurements and thus may be less accurate than those in central regions.

SD-OCT images are obtained by scanning multiple parallel lines in a rectangular scan pattern, providing a more homogeneous distribution of measured points within the macular area [39,40]. Nevertheless, the number of A-scans per line varies among different OCT scanners. It is now possible to obtain a three-dimensional image of the normal (Fig. 1.6) and diseased retina.

To evaluate and quantify macular thickening, patient's data should be compared with a normative database (defining threshold values), established in eyes with normal retinal status. However, retinal thickness measurements obtained by various OCT instruments differ, mainly due to different segmentation algorithms. Normal retinal thickness in the macular area, measured with time-domain devices, has been calculated to be 200–250 µm, and physiological foveal depression has a mean thickness of 170 µm [17, 41]. Based on these reference values, retinal thickness is considered normal, borderline, or thickened, in the setting of edema [41, 42] (Table 1.1).

Recently, Wolf-Schnurrbusch et al. [43] compared central retinal thickness (CRT) measurements (central 1,000-µm diameter area) in healthy eyes, obtained by six different commercially available OCT instruments, including time-domain and spectral-domain OCT. These authors also compared the intersession reproducibility of such measurements. Table 1.2 shows (different) CRT values of the right eye (µm ± SD).

OCT scans should be analyzed in two steps, regarding qualitative and quantitative information. Qualitative assessment relies on the characterization of the reflectivity profiles and morphological properties of the intraocular structures, whether normal or abnormal, visualized in the scans; quantitative evaluation refers to the possibility to measure these structures. After this analysis, the data should be integrated and correlated with clinical data, with previous exams and, if necessary, with

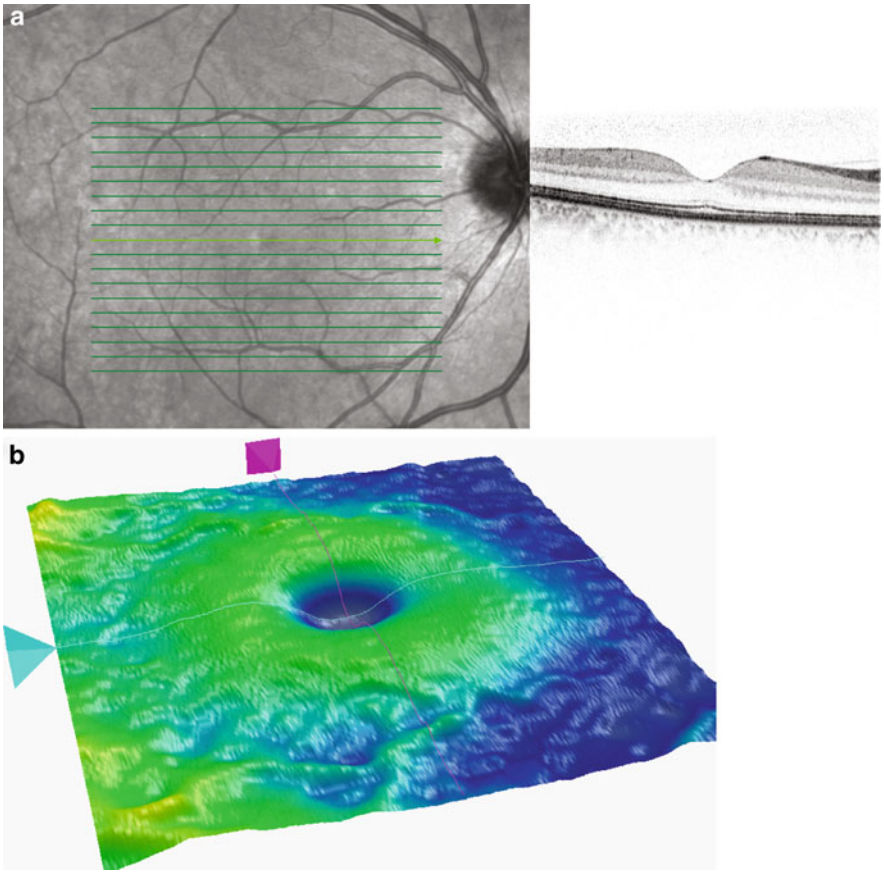

Fig. 1.6 (**a**) SD-OCT, Spectralis: acquisition protocol (parallel lines); (**b**) SD-OCT, Cirrus: 3D image of RT from a healthy volunteer

Table 1.1 Retinal thickness (RT) and standard deviation (SD) values, measured by OCT2 [41]

	RT [μm] (average ± SD)		
	Fovea	Central area (1.0 mm diameter)	Perifoveal and peripheral areas
Normal	150 ± 20	170 ± 20	230 ± 20
Borderline	170–210	190–230	250–290
Edema	≥210	≥230	≥290

information obtained by other diagnostic tools, namely, fluorescein angiography, aiming for a better correct diagnosis [17].

Reflections of the low coherent light from the ocular tissues should be differentiated between hyperreflectivity, hyporeflectivity, and shadowing effects (Table 1.3) [17].

Table 1.2 Mean CRT values (±standard deviation) obtained in central 1,000-μm diameter area [43]

Instrument	CRT [μm] (average ± SD)
Stratus OCT	212 ± 19
Spectralis HRA + OCT	289 ± 16
Cirrus HD-OCT	277 ± 19
Spectral OCT/SLO	243 ± 25
SOCT Copernicus	246 ± 23
RTVue—100	245 ± 28

Table 1.3 OCT qualitative interpretation [17]

Hyperreflectivity	Hyporeflectivity	Shadow effect
Hard exudates	Intraretinal edema	Hemorrhages
Cotton wool spots	Exudative retinal detachment	Exudates
	Cystoid macular edema	Retinal vessels

Cross-sectional images and retinal thickness measurements from various OCT devices show differences, due to different resolution, program segmentation, and/or alignment algorithms (Fig. 1.7).

Nowadays, OCT is increasingly used in the management of DME. Cross-sectional images of the retinal structures and thickness maps provide an objective and reproducible baseline characterization of the retinal disease. OCT imaging seems to be more sensitive than slit-lamp biomicroscopy to detect small changes in retinal thickness [16–18] and to visualize infraclinical foveolar detachments [19]. OCT scans also allow an accurate evaluation of disease progression, over time, and particularly after treatment.

Optical coherent tomography images of DME depict the presence of low intraretinal reflectivity, due to fluid accumulation in the extracellular space of the retina. The process begins as a diffuse retinal thickening with sponge-like appearance of the retinal layers, showing increase in the extracellular spaces advancing to the typical image of cystoid spaces [44, 45]. The hyporeflective cystoid-like cavities within the neurosensory retina are separated by highly reflective septa bridging retinal layers (Fig. 1.8a). They can progress to large and confluent hyporeflective (cystoid) spaces, involving the full thickness of the retina, with atrophy of the surrounding layers (Fig. 1.8b). Therefore, in newly developed CME, cystoid spaces are primarily located in the plexiform layer, while in well-established CME, cystoid spaces become confluent, and large cystoid cavities appear. Micropseudocysts, sometimes in the inner retina, may be identified with spectral-domain devices, even when retinal thickening is moderate, demonstrating the increase in extracellular space. They appear as small round hyporeflective lacunae with high signal elements bridging retinal layers (Fig. 1.8c) [44]. These small lesions are not visualized by time-domain OCT.

Increased thickening of the retina may also appear as an accumulation of serous fluid under the neurosensory retina, leading to a serous retinal detachment [46, 47]

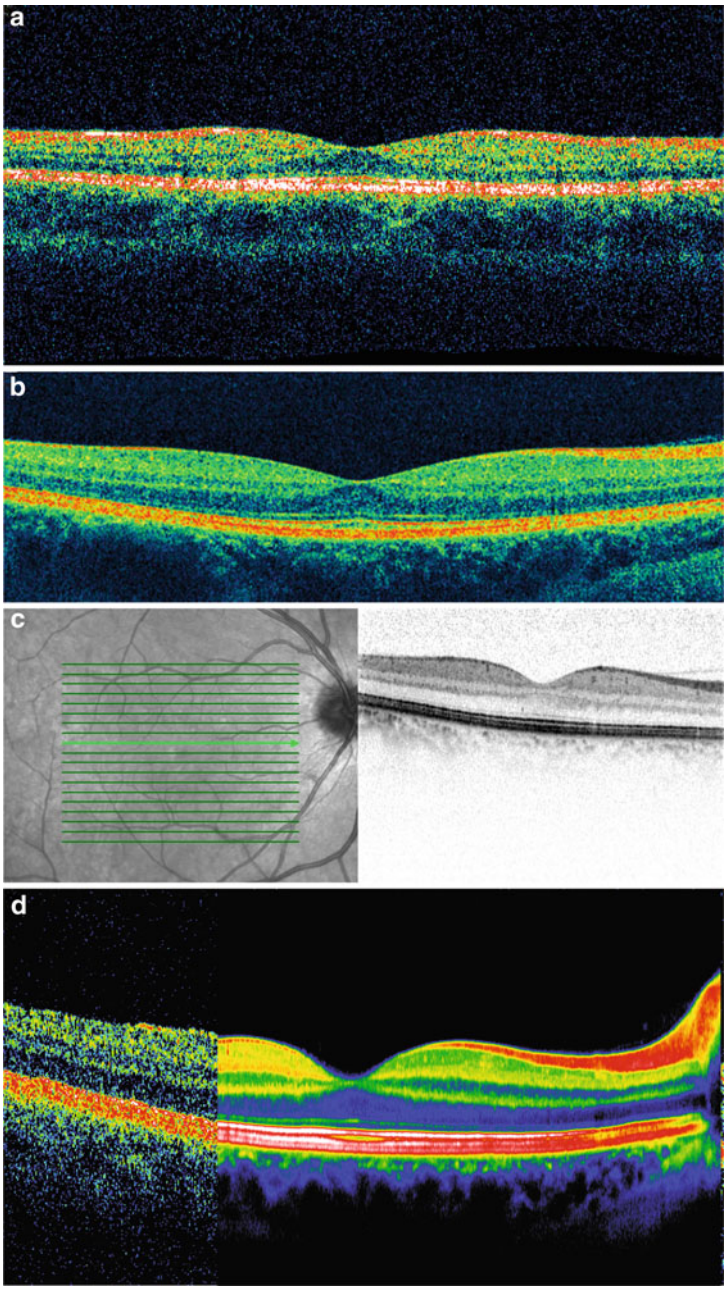

Fig. 1.7 Normal cross-sectional image of the retina. (**a**) Scan obtained with TD-OCT, Stratus; (**b**) scan obtained with SD-OCT, Cirrus; (**c**) scan obtained with SD-OCT, Spectralis (gray scale); and (**d**) comparison between scan obtained with TD-OCT (Stratus) and SD-OCT (Spectralis) (false color scale)

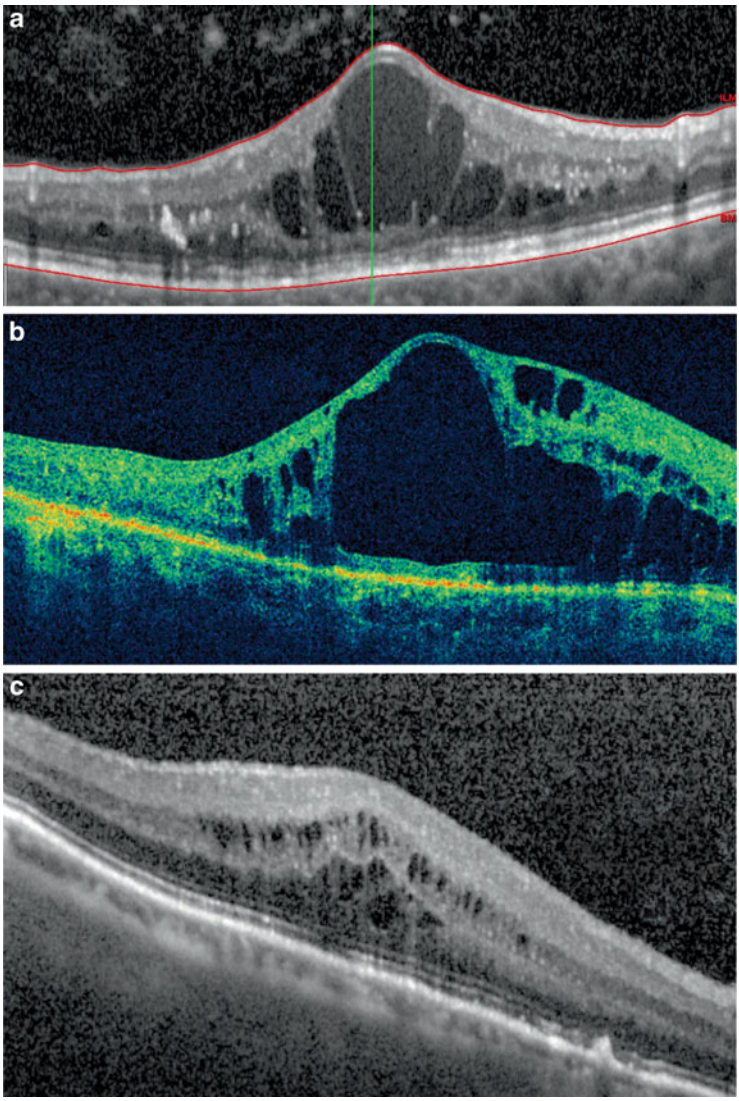

Fig. 1.8 Cystoid macular edema. (**a**) SD-OCT, Spectralis; (**b**) SD-OCT, Cirrus: confluent cystoid spaces (long-standing CME); and (**c**) SD-OCT, Spectralis: small cysts in the inner nuclear layer

(Fig. 1.9). This finding is not visible on biomicroscopy, but can be detected by OCT, as a hyporeflective area under the macula elevating the neurosensory retina above. It corresponds to an optically clear space between the retina and RPE, with a distinct outer border of the detached retina [48]. The distinction between subretinal and intraretinal fluid is possible by the identification of the highly reflective posterior

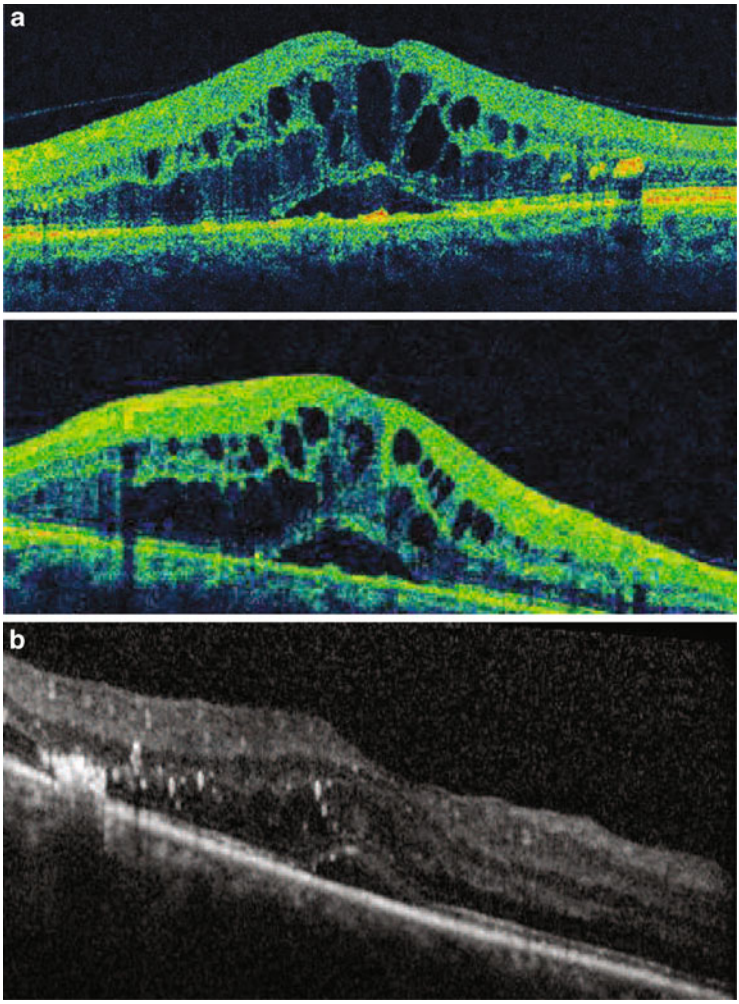

Fig. 1.9 DME with serous fluid detachment. (**a**) SD-OCT, Cirrus (*right* and *left* eye from the same patient); and (**b**) SD-OCT, Spectralis

border of the detached retina. Although there are different pathogenic mechanisms proposed for this type of edema [49–52], it may be associated with a dysfunction of the outer BRB [53, 54].

Another finding in DME is an outer retinal thickening, characterized by an ill-defined, widespread hyporeflective area, which can be distinguished from serous retinal detachment, by the absence of a highly reflective anterior boundary (Fig. 1.10).

Hard exudates are visualized as spots of high reflectivity with low reflective areas behind them (shadow effect), located in the outer retinal layers [55]

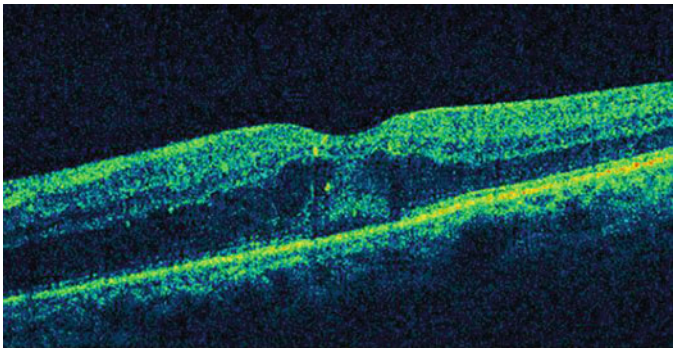

Fig. 1.10 SD-OCT, Cirrus. DME with outer retinal thickening

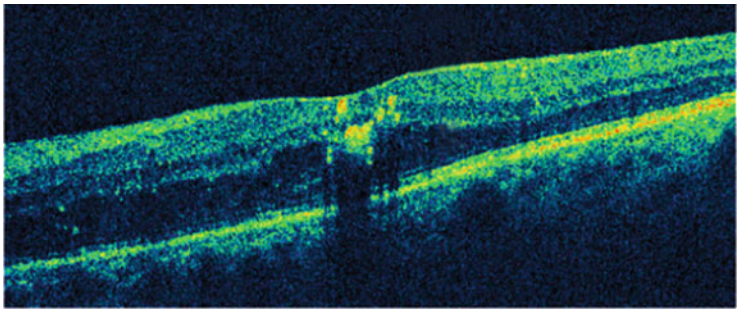

Fig. 1.11 SD-OCT, Cirrus. Hard exudates

(Figs. 1.9 and 1.11). They are due to protein or lipid deposition, secondary to the breakdown of the BRB. Hemorrhages also block the reflections from deeper retinal layers. Areas of previous focal laser treatment show an increased retinal reflectivity in the outer retinal layers (outer nuclear layer, photoreceptor layer, and retinal pigment epithelium). These morphologic changes are often associated with a decrease in central RT and thickening at the lesion site, especially in the photoreceptor layer [56].

Another advantage of the OCT is the possibility to analyze the vitreomacular interface. It is possible to determine the status of the posterior hyaloids when it is only slightly detached from the macular surface [57]. The concept of vitreoretinal traction is now considered of major relevance in the OCT classification of DME [51, 58] as it is considered to have an important role in the occurrence of ME. It appears in the OCT as a peak-shaped detachment of the retina with an area of low signal underlying the highly reflective border of the neurosensory retina, accompanied by posterior hyaloidal traction. The posterior hyaloidal traction is visible in the OCT as highly reflective signal arising from the inner retinal surface, partially detached from the posterior pole, toward to the optic nerve or peripherally, with adjacent

vitreomacular traction (Figs. 1.12 and 1.13). The vitrectomy is considered beneficial in these cases [59–62].

DME can assume different morphologic patterns on OCT [15, 44, 45]. Kim et al. [15] proposed five morphologic patterns. A modification of their classification based on OCT interpretation and relationship with predominant inner or outer BRB breakdown is followed by our group:

Patterns of macular edema:

I. – Edema of the inner retinal layers
   – Breakdown of inner/outer BRB

II. – Cystoid spaces in the retina. Overall involvement
   – Breakdown of inner/outer BRB

III. –Subretinal fluid accumulation
   – Breakdown of outer BRB

IV. – Tractional retina edema
   – Breakdown of inner BRB

V. – Combination of patterns I, II, III, IV

In summary, OCT is today the only method that allows an objective follow-up of the major characteristics of DME. It allows a clear identification of the intraretinal fluid distribution and the presence or absence of vitreous traction. It is an excellent method to document these findings. Furthermore, OCT allows a quantitative diagnosis of ME, as it is used to obtain numerical representation of the retinal thickness.

CSME may be diagnosed using only biomicroscopy, but CSME with minimal increase in retinal thickness is difficult to recognize without OCT. Different studies demonstrated that OCT may identify DME in patients with normal biomicroscopy [17, 18, 63]. In diabetic patients with increased retinal thickness between 200 and 300 μm, considering abnormal values if they are above 200 μm, only 14% are detected by ophthalmoscopy. It corresponds to a subclinical form of macular edema [64].

Macular thickening is usually topographically correlated with leakage, in fluorescein angiography [39, 64, 65]; thus, it is considered an indicator of permeability of the BRB in the macular area. This correlation is better in the area within 1,500–3,000 μm around the fovea and less clear in the central 500–1,000 μm [66]. Recent work by our group has shown that it is possible to detect the alteration of the BRB, noninvasively with OCT measurements [67].

Clinical evaluation of macular edema should include the following parameters: extension of macular edema (i.e., thickened area); location of the edema in the macular area and, particularly, central foveal involvement (central area, 500 μm wide); presence or absence of vitreous traction; and chronicity of the edema (i.e., time elapsed since initial diagnosis and response to therapy). If considered

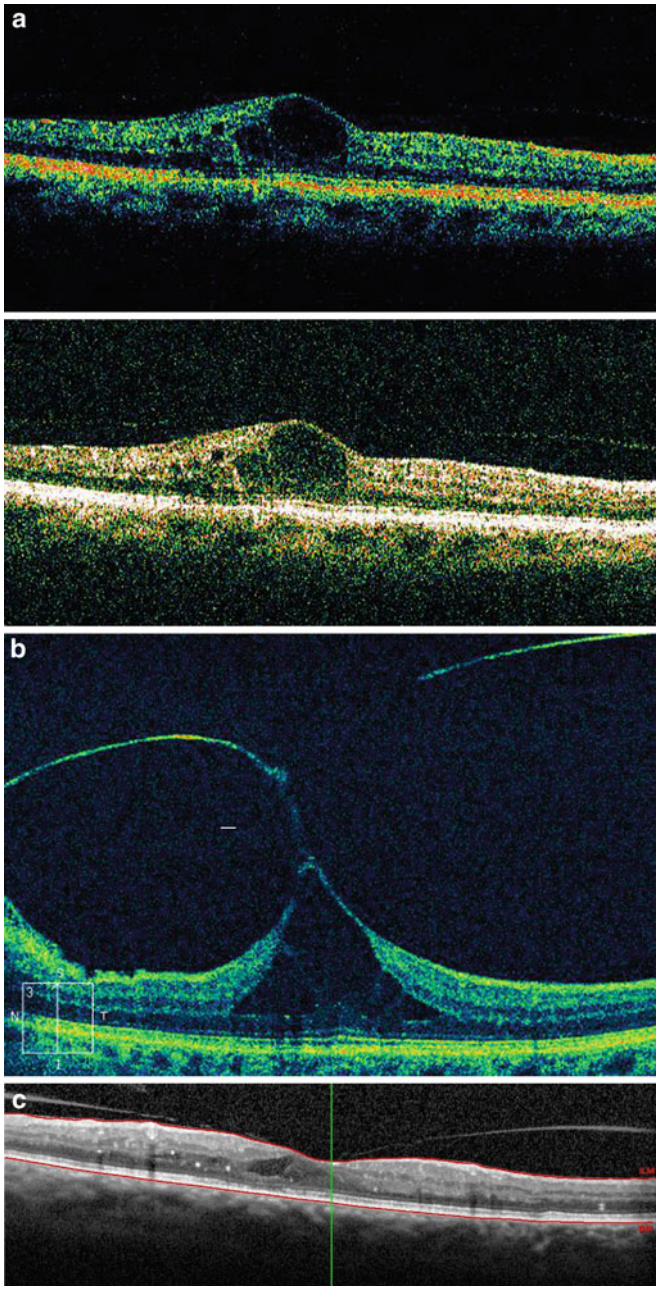

Fig. 1.12 Vitreomacular traction. (**a**) TD-OCT, Stratus (same patient); (**b**) SD-OCT, Cirrus; and (**c**) SD-OCT, Spectralis

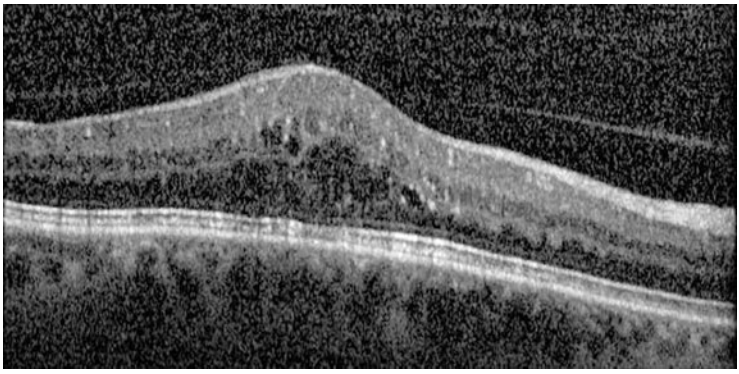

Fig. 1.13 Detachment of posterior hyaloids with vitreomacular traction. SD-OCT, Spectralis

necessary to complement the information obtained with OCT, information about the presence of ischemia may be obtained by performing fluorescein angiography.

In conclusion, OCT is a particularly valuable diagnostic tool in DME, helpful both in the diagnosis and follow-up procedure. DME classification systems should be based on OCT evaluation and measurements.

References

1. H. King, R.E. Aubert, W.H. Herman, Global burden of diabetes, 1995–2025: prevalence, numerical estimates, and projections. Diabetes Care **21**(9), 1414–1431 (1998)
2. L.P. Aiello, T.W. Gardner, G.L. King, G. Blankenship, J.D. Cavallerano, F.L.I.I.I. Ferris, R. Klein, Diabetic retinopathy. Technical review. Diabetes Care **21**, 143–156 (1998)
3. B.E. Klein, R. Klein, K.E. Lee, Components of the metabolic syndrome and risk of cardiovascular disease and diabetes in beaver dam. Diabetes Care **25**(10), 1790–1794 (2002)
4. J. Cunha-Vaz, Diabetic macular edema. Eur. J. Ophthalmol. **8**(3), 127–130 (1998)
5. J. Cunha-Vaz, A. Travassos, Breakdown of the blood-retinal barriers and cystoid macular edema. Surv. Ophthalmol. **28**(Suppl), 485–492 (1984)
6. C. Lobo, R. Bernardes, J.R. Faria de Abreu, J. Cunha-Vaz, Novel imaging techniques for diabetic macular edema. Doc. Ophthalmol. **97**, 341–347 (1999)
7. R. Klein, B. Klein, S. Moss, K. Cruickshanks, The Wisconsin Epidemiologic study of Diabetic Retinopathy XV. Ten year incidence and progression of diabetic retinopathy. Arch. Ophthalmol. **112**, 1217–1288 (1994)
8. Early Treatment Diabetic Retinopathy Study Research Group, Grading diabetic retinopathy from stereoscopic color fundus photographs—an extension of the modified Airlie House classification. ETDRS report number 10. Ophthalmology **98**(5 Suppl), 786–806 (1991)
9. Early Treatment Diabetic Retinopathy Study Group, Photocoagulation for diabetic macular edema: early treatment diabetic retinopathy study report no 1. Arch. Ophthalmol. **103**(12), 1796–1806 (1985)
10. G. Richard, G. Soubrane, L.A. Yannuzzi, *Fluorescein and ICG Angiography*,, 2nd edn. (Thieme, Stuttgart, 1998), chap. 2, pp. 15–16
11. A. Girach, H. Lund-Andersen, Diabetic macular edema: a clinical review. J. Clin. Pract. **61**, 88–97 (2007)

12. R. Klein, M.D. Knudtson, K.E. Lee, R. Gangnon, B.E. Klein, The Wisconsin Epidemiologic study of Diabetic Retinopathy XXIII: the twenty-five-year incidence of macular edema in persons with type I diabetes. Ophthalmology **116**, 497–503 (2009)
13. N. Bhagat, R.A. Grigorian, A. Tutela, M.A. Zarbin, Diabetic macular edema: pathogenesis and treatment. Surv. Ophthalmol. **54**(1), 1–32 (2009)
14. S. Yamamoto, T. Yamamoto, M. Hayashi, S. Takeuchi, Morphological and functional analyses of diabetic macular edema by optical coherence tomography and multifocal electroretinograms. Graefes Arch. Clin. Exp. Ophthalmol. **239**(2), 96–101 (2001)
15. B.Y. Kim, S.D. Smith, P.K. Kaiser, Optical coherence tomographic patterns of diabetic macular edema. Am. J. Ophthalmol. **142**(3), 405–412 (2006)
16. M.R. Hee, C.A. Puliafito, C. Wong, J.S. Duker, E. Reichel, B. Rutledge, J.S. Schuman, E.A. Swanson, J.G. Fujimoto, Quantitative assessment of macular edema with optical coherence tomography. Arch. Ophthalmol. **113**, 1019–1029 (1995)
17. G.E. Lang, Optical coherence tomography findings in diabetic retinopathy, in *Diabetic Retinopathy*, vol. 39, ed. by G.E. Lang. *Dev Ophthalmol* (Karger, Basel, 2007), pp. 31–47
18. C.S. Yang, C.Y. Cheng, F.L. Lee, W.M. Hsu, J.H. Liu, Quantitative assessment of retinal thickness in diabetic patients with and without clinically significant macular edema using optical coherence tomography. Acta Ophthalmol. Scand. **79**(3), 266–270 (2001)
19. P. Massin, A. Girach, A. Erginay, A. Gaudric, Optical coherence tomography: a key to the future management of patients with diabetic macular oedema. Acta Ophthalmol. Scand. **84**(4), 466–474 (2006)
20. R. Margolis, K. Kaiser, Diagnostic modalities in diabetic retinopathy, in *Diabetic Retinopathy—Contemporary Diabetes*, vol. 1, ed. by E.J. Duh (Humana Press, Totowa, NJ, 2008), pp. 109–133
21. J. Cunha-Vaz, G. Coscas, Diagnosis in macular edema. In: Steroids and management of macular edema. Ophthalmologica **224**(Suppl 1), 2–7 (2010)
22. W. Drexler, Cellular and functional optical coherence tomography of the human retina: the Cogan lecture 1. Invest Ophthalmol Vis Sci **48**, 5339–5351 (2007)
23. M. Pircher, E. Götzinger, O. Findl, S. Michels, W. Geitzenauer, C. Leydolt, U. Schmidt-Erfurth, C.K. Hitzenberger, Human macula investigated in vivo with polarization-sensitive optical coherence tomography. Invest. Ophthalmol. Vis. Sci. **47**, 5487–5494 (2006)
24. G. Coscas, *Optical Coherence Tomography in Age Related Macular Degeneration (OCT in AMD)*, (Springer; Edit., Heidelberg, 2009; 1389-Lamy, Publ., Marseille, 2009). ISBN 978-3-642-01468-0 (Print) 978-3-642-01467-3 (Online)
25. T. Murakami, A. Tsujikawa, M. Ohta, K. Miyamoto, M. Kita, D. Watanabe, H. Takagi, N. Yoshimura, Photoreceptor status after resolved macular edema in branch retinal vein occlusion treated with tissue plasminogen activator. Am. J. Ophthalmol. **143**(1), 171–173 (2007)
26. C.M. Eandi, J.E. Chung, F. Cardillo-Piccolino, R.F. Spaide, Optical coherence tomography in unilateral resolved central serous chorioretinopathy. Retina **25**(4), 417–421 (2005)
27. M.A. Sandberg, R.J. Brockhurst, A.R. Gaudio, E.L. Berson, The association between visual acuity and central retinal thickness in retinitis pigmentosa. Invest. Ophthalmol. Vis. Sci. **46**(9), 3349–3354 (2005)
28. L.A. Paunescu, T.H. Ko, J.S. Duker, A. Chan, W. Drexler, J.S. Schuman, J.G. Fujimoto, Idiopathic juxtafoveal retinal telangiectasis: new findings by ultrahigh-resolution optical coherence tomography. Ophthalmology **113**(1), 48–57 (2006)
29. A. Gaudric, G. Ducos de Lahitte, S.Y. Cohen, P. Massin, B. Haouchine, Optical coherence tomography in group 2A idiopathic juxtafoveal retinal telangiectasis. Arch. Ophthalmol. **124**(10), 1410–1419 (2006)
30. A.S. Maheshwary, S.F. Oster, R.M. Yuson, L. Cheng, F. Mojana, W.R. Freeman, The association between percent disruption of the photoreceptor inner segment-outer segment junction and visual acuity in diabetic macular edema. Am. J. Ophthalmol. **150**(1), 63–67 (2010)
31. H.J. Shin, S.H. Lee, H. Chung, H.C. Kim, Association between photoreceptor integrity and visual outcome in diabetic macular edema. Graefes Arch. Clin. Exp. Ophthalmol. **250**(1), 61–70 (2012)

32. F. Forooghian, P.F. Stetson, S.A. Meyer, E.Y. Chew, W.T. Wong, C. Cukras, C.B. Meyerle, F.L. Ferris 3rd, Relationship between photoreceptor outer segment length and visual acuity in diabetic macular edema. Retina **30**(1), 63–70 (2010)
33. A. Martidis, J.S. Duker, P.B. Greenberg, A.H. Rogers, C.A. Puliafito, E. Reichel, C. Baumal, Intravitreal triamcinolone for refractory diabetic macular edema. Ophthalmology **109**(5), 920–927 (2002)
34. S. Yamamoto, T. Yamamoto, M. Hayashi, S. Takeuchi, Morphological and functional analyses of diabetic macular edema by optical coherence tomography and multifocal electroretinograms. Graefes Arch. Clin. Exp. Ophthalmol. **239**(2), 96–101 (2001)
35. C. Strøm, B. Sander, N. Larsen, M. Larsen, H. Lund-Andersen, Diabetic macular edema assessed with optical coherence tomography and stereo fundus photography. Invest. Ophthalmol. Vis. Sci. **43**(1), 241–245 (2002)
36. S. Nunes, I. Pereira, A. Santos, R. Bernardes, J. Cunha-Vaz, Central retinal thickness measured with HD-OCT shows a weak correlation with visual acuity in eyes with CSME. Br. J. Ophthalmol. **94**(9), 1201–1204 (2010)
37. Diabetic Retinopathy Clinical Research Network, D.J. Browning, A.R. Glassman, L.P. Aiello, R.W. Beck, D.M. Brown, D.S. Fong, N.M. Bressler, R.P. Danis, J.L. Kinyoun, Q.D. Nguyen, A.R. Bhavsar, J. Gottlieb, D.J. Pieramici, M.E. Rauser, R.S. Apte, J.I. Lim, P.H. Miskala, Relationship between optical coherence tomography-measured central retinal thickness and visual acuity in diabetic macular edema. Ophthalmology **114**(3), 525–536 (2007)
38. M.R. Hee, C.A. Puliafito, C. Wong, J.S. Duker, E. Reichel, B. Rutledge, J.G. Coker, J.R. Wilkins, J.S. Schuman, E.A. Swanson, J.G. Fujimoto, Topography of diabetic macular edema with optical coherence tomography. Ophthalmology **105**(2), 360–370 (1998)
39. P. Massin, E. Vicaut, B. Haouchine, A. Erginay, M. Paques, A. Gaudric, Reproducibility of retinal mapping using optical coherence tomography. Arch.Ophthalmol. **119**, 1135–1142 (2001)
40. A. Polito, M. Del Borrello, M. Isola, N. Zemella, F. Bandello, Repeatability and reproducibility of fast macular thickness mapping using stratus optical coherence tomography. Arch. Ophthalmol. **123**(10), 1330–1337 (2005)
41. G. Panozzo, B. Parolini, E. Gusson, A. Mercanti, S. Pinackatt, G. Bertolo, S. Pignatto, Diabetic macular edema: an OCT-based classification. Semin. Ophthalmol. **19**(1–2), 13–20 (2004)
42. R. Brancato, B. Lumbroso, *Guide to Optical Tomography Interpretation* (Innovation-News Communication, Rome, 2004)
43. U. Wolf-Schnurrbusch, L. Ceklic, C.K. Brinkmann, M. Iliev, M. Frey, S. Rothenbuehler, V. Enzmann, S. Wolf, Macular Thickness measurements in healthy eyes using six different optical coherence tomography instruments. Invest. Ophthalmol. Vis. Sci. **50**(7), 3432–3437 (2009)
44. T. Otani, S. Kishi, Y. Mauyama, Patterns of diabetic macular edema with optical coherence tomography. Am. J. Ophthalmol. **127**(6), 688–693 (1999)
45. H. Alkuraya, D. Kangave, A.M. Abu El-Asrar, The correlation between coherence tomography features and severity of retinopathy, macular thickness and visual acuity in diabetic macular edema. Int. Ophthalmol. **26**(3), 93–99 (2005)
46. H. Ozdemir, M. Karacorlu, S. Karacorlu, Serous macular detachment in diabetic cystoid macular oedema. Acta Ophthalmol. Scand. **83**, 63–66 (2005)
47. A. Catier, R. Tadayoni, M. Paques, A. Erginay, B. Haouchine, A. Gaudric, P. Massin, Optical coherence tomography characterization of macular edema according to various etiology. Am. J. Ophthalmol. **140**(2), 200–206 (2005)
48. G.H. Bresnick, Diabetic macular edema: a review. Ophthalmology **93**(7), 989–997 (1986)
49. T. Otani, S. Kishi, Topographic assessment of vitreous surgery for diabetic macular edema. Am. J. Ophthalmol. **129**, 487–494 (2000)
50. T. Nagaoka, N. Kitaya, R. Sugawara, Alteration of choroidal circulation in the foveal region in patients with type II diabetes. Br. J. Ophthalmol. **88**(8), 1060–1063 (2004)
51. S. Kang, C. Yon Park, D. Ham, The correlation between fluorescein angiography and optical coherence tomography features in clinically significant macular edema. Am. J. Ophthalmol. **137**(2), 313–322 (2004)

52. W. Soliman, B. Sancher, T. Martini, Enhanced optical coherence patterns of diabetic macula edema and the correlation with the pathophysiology. Acta Ophthalmol. Scand. **85**(6), 613–617 (2007)
53. D. Gaucher, C. Sebah, A. Erginay, B. Haoucine, R. Tadayoni, A. Gaudric, P. Massin, Optical coherence tomography features during the evolution of serous retinal detachment in patients with macular edema. Am. J. Ophthalmol. **145**(2), 289–296 (2008)
54. F. Bandello, M. Battaglia Parodi, P. Lanzetta, A. Loewenstein, P. Massin, F. Menchini, D. Veritti, Diabetic macular edema, in *Macular Edema*, vol. 47, ed. by G. Coscas. *Dev Ophthalmol* (Karger, Basel, 2010), pp. 73–110
55. M. Bolz, U. Schmidt-Erfurth, G. Deak, G. Mylonas, K. Kriechbaum, C. Scholda, Optical coherence tomographic hyperreflective foci: a morphologic sign of lipid extravasation in diabetic macular edema. Ophthalmology **116**(5), 914–920 (2009)
56. M. Bolz, K. Kriechbaum, C. Simader, G. Deak, J. Lammer, C. Treu, C. Scholda, C. Prünte, U. Schmidt-Erfurth, Diabetic Retinopathy Research Group Vienna. In vivo retinal morphology after grid laser treatment in diabetic macular edema. Ophthalmology **117**(3), 538–554 (2010)
57. D. Gaucher, R. Tadayoni, A. Erginay, B. Haouchine, A. Gaudric, P. Massin, Optical coherence tomography assessment of the vitreoretinal relationship in diabetic macular edema. Am. J. Ophthalmol. **139**(5), 807–813 (2005)
58. G. Panozzo, E. Gusson, B. Parolini, A. Mercanti, Role of OCT in diagnosis and follow up of diabetic macular edema. Semin. Ophthalmol. **18**(2), 74–81 (2003)
59. H. Lewis, G.W. Abrams, M.S. Blumen Krans, R.V. Campo, Vitrectomy for diabetic macular traction and edema associated with posterior hyaloid traction. Ophthalmology **99**, 753–759 (1992)
60. P. Massin, G. Duguid, A. Erginay, B. Haouchine, A. Gaudric, Optical coherence tomography for evaluating diabetic macular edema before and after vitrectomy. Am. J. Ophthalmol. **135**(2), 169–177 (2003)
61. D. Thomas, C. Bunce, C. Moorman, A.H. Laidlaw, Frequency and associations of a taut thickened posterior hyaloid, partial vitreomacular separation, and subretinal fluid in patients with diabetic macular edema. Retina **25**(7), 883–888 (2005)
62. S.D. Pendergast, T.S. Hassan, G.A. Williams, M.S. Cox, R.R. Margherio, P.J. Ferrone, B.R. Garretson, M.T. Trese, Vitrectomy for diffuse diabetic macular edema associated with taut premacular posterior hyaloid. Am. J. Ophthalmol. **130**(2), 178–186 (2000)
63. U.H. Schaudig, C. Glaefke, F. Scholz, G. Richard, Optical coherence tomography for retinal thickness measurement in diabetic patient without clinical significant macular edema. Ophthalmic Surg. Lasers. **31**(3), 182–186 (2000)
64. J.C. Brown, S.D. Solomon, S.B. Bressler, A.P. Schachat, C. DiBernardo, N. Bressler, Detection of diabetic foveal edema, contact lens biomicroscopy compared with optical coherence tomography. Arch Ophthalmol. **122**(3), 330–335 (2004)
65. W. Goebel, T. Kretzchmar-Gross, Retinal thickness in diabetic retinopathy. A study using optical coherence tomography (OCT). Retina **22**(6), 759–767 (2002)
66. A. Neubauer, C. Chryssafis, S. Priglinger, C. Haritoglou, M. Tiel, V. Welge-Luben, A. Kampik, Topography of diabetic macular edema compared with fluorescein angiography. Acta Ophthalmol. Scand. **85**(1), 32–39 (2007)
67. R. Bernardes, T. Santos, P. Serranho, C. Lobo, J. Cunha-Vaz, Noninvasive evaluation of retinal leakage using optical coherence tomography. Ophthalmologica **226**(2), 29–36 (2011)

http://www.springer.com/978-3-642-27409-1

Optical Coherence Tomography
A Clinical and Technical Update
Bernardes, R.; Cunha-Vaz, J. (Eds.)
2012, XV, 255 p., Hardcover
ISBN: 978-3-642-27409-1